

Miscellaneous observations of active galactic nuclei. II. ^{*}

A. C. Gonçalves, P. Véron and M.-P. Véron-Cetty

Observatoire de Haute Provence (CNRS), F-04870 Saint Michel l'Observatoire, France

Received 20 March 1997 / Accepted 22 April 1997

Abstract. We observed 37 AGN candidates and classified them on the basis of their spectroscopic properties; three are confirmed QSOs, one is a BL Lac object, nine are Seyfert 1 galaxies, four Seyfert 2s, while twenty are HII regions.

Key words: Galaxies: active – Galaxies: nuclei – Galaxies: Seyfert – Galaxies: BL Lacertae objects: general – Galaxies: quasars: general – Galaxies: starburst

1. Introduction

In the course of several observing runs, we obtained optical spectra of 37 AGN candidates with uncertain classification. Twenty of them turned out to be extragalactic HII regions ionized by hot stars, while seventeen were confirmed to be QSOs, BL Lac or Seyfert galaxies. In a previous paper (Véron-Cetty & Véron, 1986), the classification of 61 AGN candidates was given.

2. Observations

Most of the observations were carried out in 1995, 1996 and 1997 with the spectrograph CARELEC (Lemaître et al., 1989) attached to the Cassegrain focus of the Observatoire de Haute Provence (OHP) 1.93m telescope. The spectrograph settings used during these runs are given in Table 1. The detector was a 512×512 pixels, $27 \times 27 \mu\text{m}$ Tektronic CCD. The slit width was 2.1 arcsec, corresponding to a projected slit width on the detector of $52 \mu\text{m}$, or 1.9 pixel. The resolution, as measured on the night sky emission lines, was 13.5 and 3.4 \AA FWHM at low and

high resolution, respectively. The spectra were flux calibrated using the standard stars given in Table 1, taken from Oke (1974), Stone (1977), Oke & Gunn (1983) or Massey et al. (1988).

Additional observations were made with EFOSC (Dekker et al., 1988) at the 3.6m ESO telescope in La Silla during two runs in July 1995 and August 1996. The detector was the CCD ESO#26, similar to the one used at OHP. The dispersion was 230 \AA mm^{-1} ; the slit width was 1.5 arcsec, corresponding to 2.2 pixels and resulting in a resolution of 15 \AA . The wavelength range was $\lambda\lambda 3500 - 7600 \text{ \AA}$. The spectra were flux calibrated using the standard stars W 485A and GD 190 (Oke, 1974).

| Date | Dispersion (\AA mm^{-1}) | λ Range (\AA) | Standard stars |
|------------------|--|-------------------------------------|--------------------------|
| 21 – 23.03.95 | 66 | 6500 – 7400 | BD 26°2606 |
| 24 – 28.08.95 | 260 | 4500 – 8000 | BD 25°3941 BD 28°4211 |
| 28 – 31.08.95 | 66 | 6700 – 7600 | BD 25°3941 BD 28°4211 |
| 31.08 – 04.09.95 | 66 | 4860 – 5760 | Feige 15 BD 28°4211 |
| 10.05.96 | 66 | 6700 – 7600 | GD 140 BD 26°2606 |
| 13.05.96 | 66 | 4860 – 5760 | Feige 98 Kopff 27 |
| 08.06.96 | 66 | 4860 – 5760 | Feige 66 Kopff 27 |
| 09.06.96 | 66 | 6700 – 7600 | Feige 66 BD 28°4211 |
| 06 – 08.01.97 | 66 | 4720 – 5620 | EG 247 |
| 08 – 11.01.97 | 66 | 6175 – 7075 | EG 247 |

Table 1. Spectrograph settings and standard stars during OHP observations.

Send offprint requests to: P. Véron

* Based on observations collected at the Observatoire de Haute-Provence (CNRS), France, and at the European Southern Observatory, La Silla, Chili.

| Name | Disp. | Date | Exp. time (min) | Name | Disp. | Date | Exp. time (min) |
|------------------|-------|----------|--------------------|-------------------|-------|----------|--------------------|
| 4C 12.05 | D | 10.08.96 | 10 | PKS 1420 – 27 | D | 25.07.95 | 10 |
| Mark 1147 | A | 26.08.95 | 20 | Mark 816 | B | 13.05.96 | 20 |
| Mark 971 | B | 01.09.95 | 20 | PKS 1437 – 153 | D | 27.07.95 | 10 |
| Mark 998 | A | 26.08.95 | 20 | Mark 833 | C | 22.03.95 | 20 |
| Q 0155 + 0220 | B | 31.08.95 | 20 | Mark 483 | C | 22.03.95 | 20 |
| Mark 596 | A | 25.08.95 | 20 | KUV 15519 + 2144 | C | 22.03.95 | 20 |
| KUV 03079 – 0101 | A | 27.08.95 | 20 | Q 1619 + 3752 | B | 01.09.95 | 20 |
| CBS 74 | A | 30.04.95 | 15 | EXO 1622.0 + 2611 | C | 22.03.95 | 20 |
| | C | 22.03.95 | 20 | Q 1624 + 4628 | C | 28.08.95 | 20 |
| HS 0843 + 2533 | C | 10.01.97 | 20 | Q 1638 + 4634 | A | 27.08.95 | 20 |
| Mark 391 | B | 07.01.97 | 20 | Kaz 110 | B | 23.06.96 | 20 |
| | C | 10.01.97 | 20 | | C | 22.06.96 | 20 |
| KUG 0929 + 324 | C | 21.03.95 | 20 | PKS 1903 – 80 | D | 28.07.95 | 10 |
| CG 49 | C | 10.05.96 | 20 | RN 73 | B | 31.08.95 | 20 |
| UM 446 | C | 21.03.95 | 20 | | C | 30.08.95 | 20 |
| US 2896 | C | 22.03.95 | 20 | Q 2233 + 0123 | C | 30.08.95 | 20 |
| Mark 646 | C | 22.03.95 | 20 | Q 2257 + 0221 | B | 02.09.95 | 20 |
| 2E 1219 + 0447 | C | 22.03.95 | 20 | NGC 7678 | B | 02.09.95 | 20* |
| KUV 13000 + 2908 | C | 22.03.95 | 20 | | C | 30.08.95 | 20 |
| Q 1356 – 067 | C | 22.03.95 | 20 | E 2344 + 184 | B | 01.09.95 | 20 |
| Mark 469 | B | 08.06.96 | 20 | UM 11 | B | 02.09.95 | 20* |
| | C | 09.06.96 | 20 | | C | 29.08.95 | 20 |

Table 2. Journal of observations. A: OHP, 260 Åmm⁻¹; B: OHP, 66 Åmm⁻¹ blue; C: OHP, 66 Åmm⁻¹ red; D: ESO, 230 Åmm⁻¹. An “*” after the exposure time indicates the presence of clouds during the exposure.

The journal of observations is given in Table 2 and the list of the observed objects with relevant data, in Table 3. The spectra were analysed in terms of Gaussian components as described in Véron et al. (1997). Table 4 gives for each object the velocity, width and relative strength of each line, together with the adopted classification. Objects with broad Balmer lines were classified as Seyfert 1 galaxies, or QSOs whenever their absolute magnitude was brighter than $M_B = -23.0$ (assuming $H_0 = 50 \text{ kms}^{-1}\text{Mpc}^{-1}$); Seyfert 2s and HII regions were distinguished on the basis of the value of the $[\text{OIII}]\lambda 5007/\text{H}\beta$ and $[\text{NII}]\lambda 6584/\text{H}\alpha$ line ratios (Veilleux and Osterbrock, 1987). In some cases, the classification is based on a single line ratio, either $\lambda 5007/\text{H}\beta$ or $\lambda 6584/\text{H}\alpha$. This is potentially dangerous; however we think that in most cases, there is no ambiguity, specially when $\lambda 6584/\text{H}\alpha < 0.3$ (see Fig. 6a in Véron et al., 1997).

3. Notes on individual objects

4C 12.05 (Gower et al., 1967) = PKS 0035+121 (Shimmins et al., 1975) has been tentatively identified by Wills & Wills (1976) and Jauncey et al. (1978) with a 16.5-17.0 mag object, the position of which is in good agreement with the accurate radio position measured by Condon et al. (1977); but they have shown that the optical spectrum, although inconclusive, was probably that of a star. How-

ever, Wills & Wills have remarked that there appears to be a small, fainter, south-preceding blue object, visible on the Palomar Sky Survey prints, blended with the image of the star. A V image, obtained on August 10, 1996 with EFOSC at the 3.6m ESO telescope on La Silla shows that, indeed, the object is double, with a separation of 2.8 arcsec. The spectrograph slit was aligned on the two objects (PA=229°); a 10 min exposure spectrum shows the north-following object to be a star, while the south-preceding object is a QSO at $z=1.395$ (Fig. 1). The magnitude of the QSO, as measured on the spectrum is about 0.55 mag weaker than the star in B, and 0.87 mag in V. The emission line fluxes are 570 and 360 $10^{-16} \text{ ergs}^{-1} \text{ cm}^{-2}$ for $\text{CIII}]\lambda 1909$ and $\text{MgII} \lambda 2798$ respectively.

Mark 1147 is an emission line galaxy (Markarian et al., 1980); it has been erroneously classified as a Seyfert 1 by Véron-Cetty & Véron (1985). Our low dispersion spectrum (Fig. 2) shows that it is a HII region, with $\lambda 5007/\text{H}\beta = 2.18$ and $\lambda 6584/\text{H}\alpha = 0.24$; this is in agreement with Markarian et al. (1980), who have noticed that $\lambda 6584$ is weak compared to $\text{H}\alpha$.

Mark 971 = KUG 0101+353 (Takase & Miyauchi-Isobe, 1991b). Markarian et al. (1984) suggested that it could have an active nucleus; this, however, was not confirmed neither by Denisyuk & Lipovetski (1984) nor by Lipovetski et al. (1989). Our spectrum (Fig. 6) shows narrow emission lines ($< 280 \text{ kms}^{-1}$ FWHM) with

$\lambda 5007/H\beta = 0.41$ together with an $H\beta$ line in absorption; this object is, therefore, a HII region.

Mark 998. According to Markarian et al. (1984), this galaxy could have an active nucleus; Denisyuk & Lipovetski (1984) and Lipovetski et al. (1989) were not able to confirm this. Our low dispersion spectrum (Fig. 2) shows $\lambda 6584/H\alpha = 0.23$. It follows that this object is most probably a HII region.

Q 0155+0220 is an emission line galaxy according to Schneider et al. (1994). Our spectrum (Fig. 6) shows it to be a HII region with narrow ($\text{FWHM} < 325 \text{ km s}^{-1}$) $H\beta$ and $\lambda 5007$ emission lines, and $\lambda 5007/H\beta = 0.71$.

Mark 596. This object, having $\lambda 6584/H\alpha > 1$ may have an active nucleus (Markarian et al., 1984). It is indeed a Seyfert 2 galaxy as our spectrum (Fig. 2) shows that $\lambda 5007/H\beta > 5$ and $\lambda 6584/H\alpha = 1.14$.

KUV 03079-0101 (Noguchi et al., 1980) is an emission line galaxy according to Chaffee et al. (1991). Our spectrum (Fig. 3) shows broad Balmer lines (3000 km s^{-1} FWHM) and narrow [OIII] lines. The ratio of the total $H\beta$ flux to the $\lambda 5007$ flux is $R=10$; this object is therefore a Seyfert 1.0 galaxy (Winkler, 1992).

CBS 74 is a Seyfert galaxy according to Wagner et al. (1988). It was not detected at 4850 MHz by Gregory & Condon (1991) ($S < 25 \text{ mJy}$) and is therefore a radioquiet object. Our spectra (Fig. 3, 9) show that it is a Seyfert 1.2 galaxy with a very broad $H\alpha$ component ($\text{FWHM} \sim 12000 \text{ km s}^{-1}$) and $R=3.6$. Such broad lines are common in radioloud quasars and broad line radiogalaxies (Miley & Miller, 1979; Wills & Browne, 1986; Brotherton et al., 1994; Eracleous & Halpern, 1994), but they are rare in Seyfert galaxies although a few cases are known, such as 2E 0450-1816 (Eracleous & Halpern, 1994) and Arp 102B (Chen & Halpern, 1989). Indeed, powerful radiogalaxies and radioloud quasars with extended radio morphologies tend to have the broadest Balmer lines, while AGNs with compact radiostructure and radioquiet objects have narrower Balmer lines (Miley & Miller, 1979; Steiner, 1981; Wills & Browne, 1986).

HS 0843+2533. The ROSAT X-ray source RX J08469+2522 was identified by Bade et al. (1995) with a 16.8 mag AGN called HS 0843+2533, which exhibits a broad $H\alpha$ emission line ($\text{FWHM} = 5900 \text{ km s}^{-1}$). Our spectrum (Fig. 9) shows, indeed, a strong, broad $H\alpha$ emission line ($\text{FWHM} = 4850 \text{ km s}^{-1}$); this object is therefore a Seyfert 1 galaxy.

Mark 391 = NGC 2691 is a S0a galaxy (Huchra, 1977). For Arakelian et al. (1972), it weakly shows the characteristics of the Seyfert nuclei, with a broad $H\alpha$ emission line ($\sim 50\text{\AA}$). On this basis, Véron-Cetty & Véron (1985) classified it as a Seyfert 1. Shuder & Osterbrock (1981), however, concluded from their own spectroscopic observations that it is not a Seyfert. Our spectra (Fig. 4) show Balmer lines in absorption together with narrow ($\text{FWHM} < 215 \text{ km s}^{-1}$) emission lines with

$\lambda 5007/H\beta = 1.21$ and $\lambda 6584/H\alpha = 0.55$, proving that it is a HII region.

KUG 0929+324 is a moderate excitation ($\lambda 5007/H\beta = 2.68$) emission line galaxy with an heliocentric radial velocity $V = 1500 \pm 70 \text{ km s}^{-1}$ according to Augarde et al. (1994). Our spectrum (Fig. 7) shows that it is a HII region with narrow emission lines ($\text{FWHM} < 150 \text{ km s}^{-1}$) and $\lambda 6584/H\alpha = 0.10$. We found the radial velocity to be $V = 4740 \text{ km s}^{-1}$ (Augarde, 1995, private communication, gave $V = 4478 \text{ km s}^{-1}$).

CG 49. Salzer et al. (1995) published line intensity ratios for this object as follows: $\lambda 5007/H\beta = 11.68$ and $\lambda 6584/H\alpha = 0.30$. The $\lambda 6584$ line is too strong for a HII region and too weak for a Seyfert 2 galaxy. Our spectrum shows $\lambda 6584$ with the same low intensity, however it so happens that the redshifted wavelength of the $\lambda 6584$ line (6874\AA) falls precisely at the position of the atmospheric B band. When corrected for atmospheric absorption by dividing the observed spectrum by the spectrum of a standard star (Fig. 7), we obtain $\lambda 6584/H\alpha = 0.79$, a normal value for a Seyfert 2 galaxy. The measured FWHM of the emission lines is $\sim 300 \text{ km s}^{-1}$, in agreement with the adopted classification.

UM 446 is a moderate excitation ($\lambda 5007/H\beta = 4.54$) emission line galaxy (Salzer et al., 1989). Our spectrum (Fig. 7) shows narrow emission lines ($\text{FWHM} < 160 \text{ km s}^{-1}$) with $\lambda 6584/H\alpha = 0.04$; this object is therefore a HII region.

US 2896 (Huang & Usher, 1984) = CS 109 (Sanduleak & Pesch, 1984) is an emission line galaxy (Mitchell et al., 1984), and a Seyfert 1.5 galaxy according to Everett & Wagner (1995). This is confirmed by our spectrum (Fig. 7) which shows a broad $H\alpha$ component (2100 km s^{-1} FWHM). A [OI] $\lambda 6300$ emission line is observed with $\lambda 6300/H\alpha_{\text{narrow}} = 0.03$.

Mark 646, PG 1203+35 (Green et al., 1986), CG 885 (Pesch & Sanduleak, 1988) or KUG 1203+354 (Takase & Miyauchi-Isobe, 1991a) is a Seyfert galaxy according to Green et al. (1986). Our spectrum (Fig. 7) shows a broad $H\alpha$ component (2350 km s^{-1} FWHM); Mark 646 is therefore a Seyfert 1 galaxy. A $\lambda 6300$ emission line is observed with $\lambda 6300/H\alpha_{\text{narrow}} = 0.05$.

2E 1219+0447 is an emission line galaxy (Bothun et al., 1984; Margon et al., 1985). We classify it as a Seyfert 1 galaxy on the basis of a weak, broad ($\text{FWHM} \sim 8500 \text{ km s}^{-1}$) $H\alpha$ component (Fig. 9).

KUV 13000+2908 (Noguchi et al., 1980), CG 963 (Sanduleak & Pesch, 1990) or PB 3241 (Berger et al., 1991) is a Seyfert 2 galaxy according to Wegner & McMahon (1988). Our spectrum (Fig. 7) shows narrow ($\text{FWHM} < 185 \text{ km s}^{-1}$) emission lines with $\lambda 6584/H\alpha < 0.1$, so this object is a HII region.

Q 1356-067 is a QSO according to Goldschmidt et al. (1992). Our spectrum (Fig. 8), however, shows narrow ($\text{FWHM} < 280 \text{ km s}^{-1}$) emission lines with $\lambda 6584/H\alpha =$

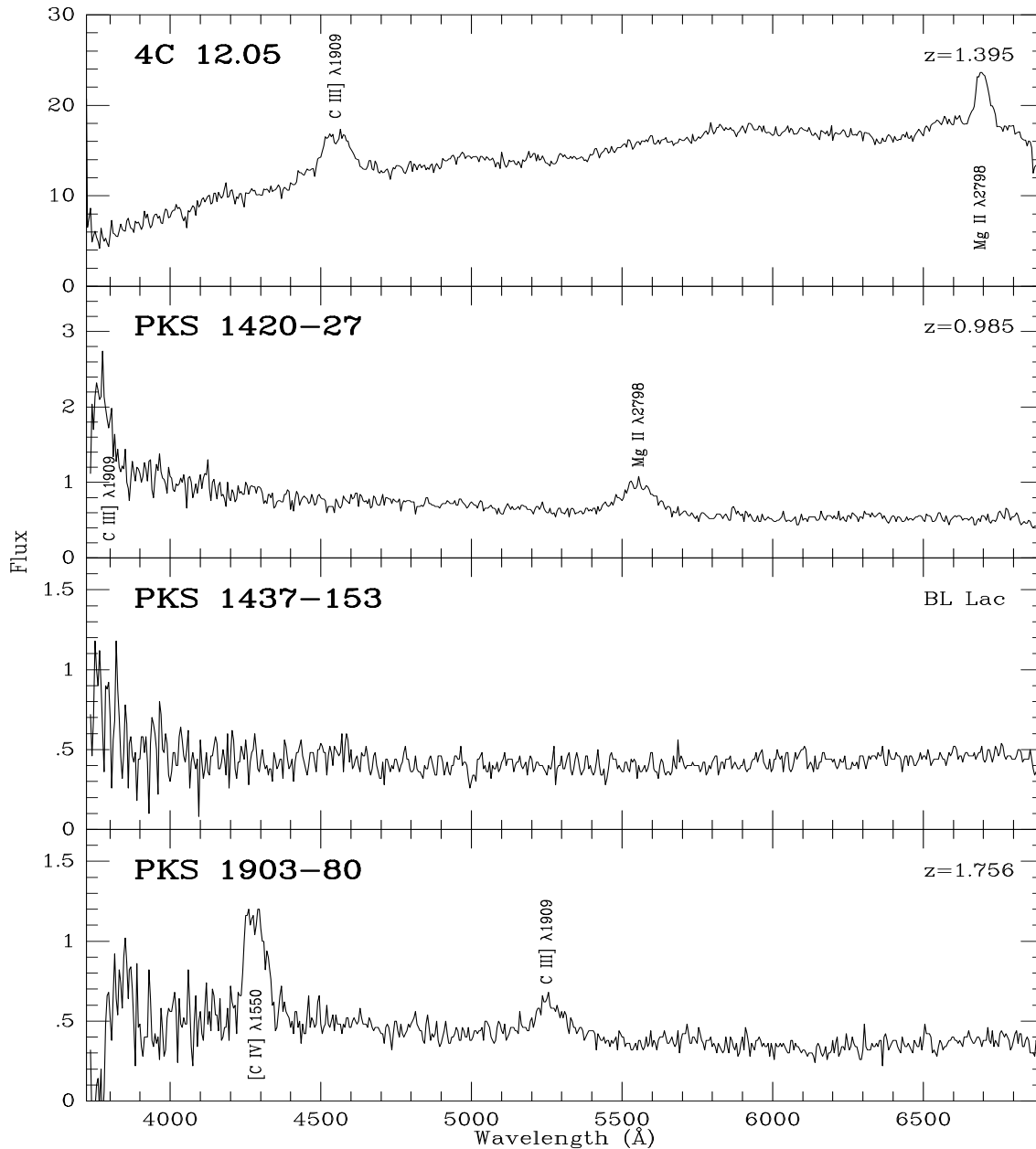


Fig. 1. Low dispersion spectra (resolution $\sim 15 \text{ \AA}$) of four objects observed with the 3.6m ESO telescope. The fluxes are in units of $10^{-16} \text{ erg s}^{-1} \text{ cm}^{-2} \text{ \AA}^{-1}$.

0.16; this object is therefore a HII region. A $\lambda 6300$ emission line is observed with $\lambda 6300/H\alpha = 0.015$

$\lambda 5007/H\beta = 1.38$ and $\lambda 6584/H\alpha = 0.18$, the lines being narrow ($\text{FWHM} < 260 \text{ km s}^{-1}$).

Mark 469, CG 899 (Pesch & Sanduleak, 1989) or KUG 1416+345 (Takase & Miyauchi-Isobe, 1984) is a 16.1 mag, UV excess galaxy (Peterson et al., 1981). Our observations (Fig. 4) show that it is a HII region, with

PKS 1420-27. This radiosource was identified by Bolton & Ekers (1966) with an 18 mag QSO. The identification was later confirmed by accurate optical and radio position measurements (Hunstead 1971, 1972). Our spec-

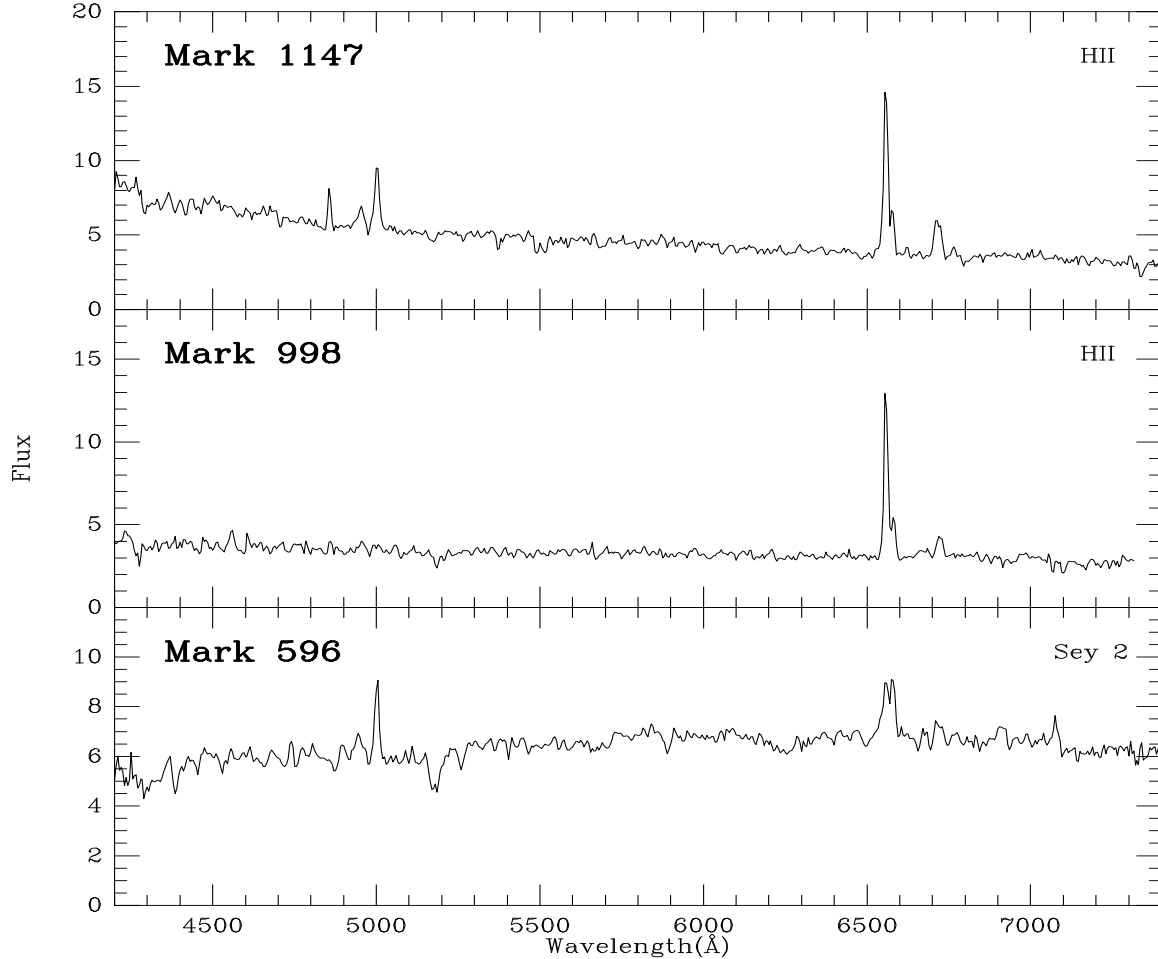


Fig. 2. Low dispersion spectra (resolution $\sim 13.5 \text{ \AA}$), in the rest frame, of three objects observed with the 1.93m OHP telescope. The fluxes are in units of $10^{-16} \text{ erg s}^{-1} \text{ cm}^{-2} \text{ \AA}^{-1}$.

trum (Fig. 1) shows that it is indeed a QSO at $z = 0.985$. The emission line fluxes are 83 and $53 \text{ } 10^{-16} \text{ erg s}^{-1} \text{ cm}^{-2}$ for $\text{CIII]}\lambda 1909$ and $\text{MgII } \lambda 2798$ respectively.

Mark 816 = KUG 1431+529 (Takase & Miyauchi-Isobe, 1985) is a 16.5 mag, possibly Seyfert, galaxy (Afanasev et al., 1979); however, $\lambda 6584/\text{H}\alpha < 0.3$ (Afanasev et al., 1980). Our spectrum (Fig. 6) shows narrow emission lines ($< 240 \text{ km s}^{-1}$ FWHM) with $\lambda 5007/\text{H}\beta = 0.63$. This object is most probably a HII region.

PKS 1437-153 is a flat spectrum radio source identified by Condon et al. (1977) with a 19.0 mag starlike object. It has a featureless spectrum between 3800 and 7000 \AA (Fig. 1) and is most probably a BL Lac object.

Mark 833 = CG 590 (Sanduleak & Pesch, 1987) is an emission line galaxy (Markarian et al., 1985) which

has been called a "narrow-line active galactic nucleus" by Veilleux & Osterbrock (1987), based on emission-line intensity ratios published by Shuder & Osterbrock (1981); it however happened that the object studied in this last paper is Mark 883 which is, in a few occasions mistakenly called Mark 833 (H. Falcke, private communication). The nature of the emission-line nebulosity in Mark 833 was therefore unknown. Our spectrum (Fig. 8) shows narrow (FWHM $< 225 \text{ km s}^{-1}$) emission lines with $\lambda 6584/\text{H}\alpha = 0.30$. This object is, therefore, a HII region.

Mark 483 = CG 741 (Sanduleak & Pesch, 1987) is an emission line galaxy (Markarian et al., 1988; Izotov et al., 1993) with a strong UV excess ($U-B = -0.45$, Peterson et al., 1981). The emission-line ratios published by Markarian et al. ($\lambda 6584/\text{H}\alpha < 0.33$) and Izotov et al. ($\lambda 5007/\text{H}\beta \sim$

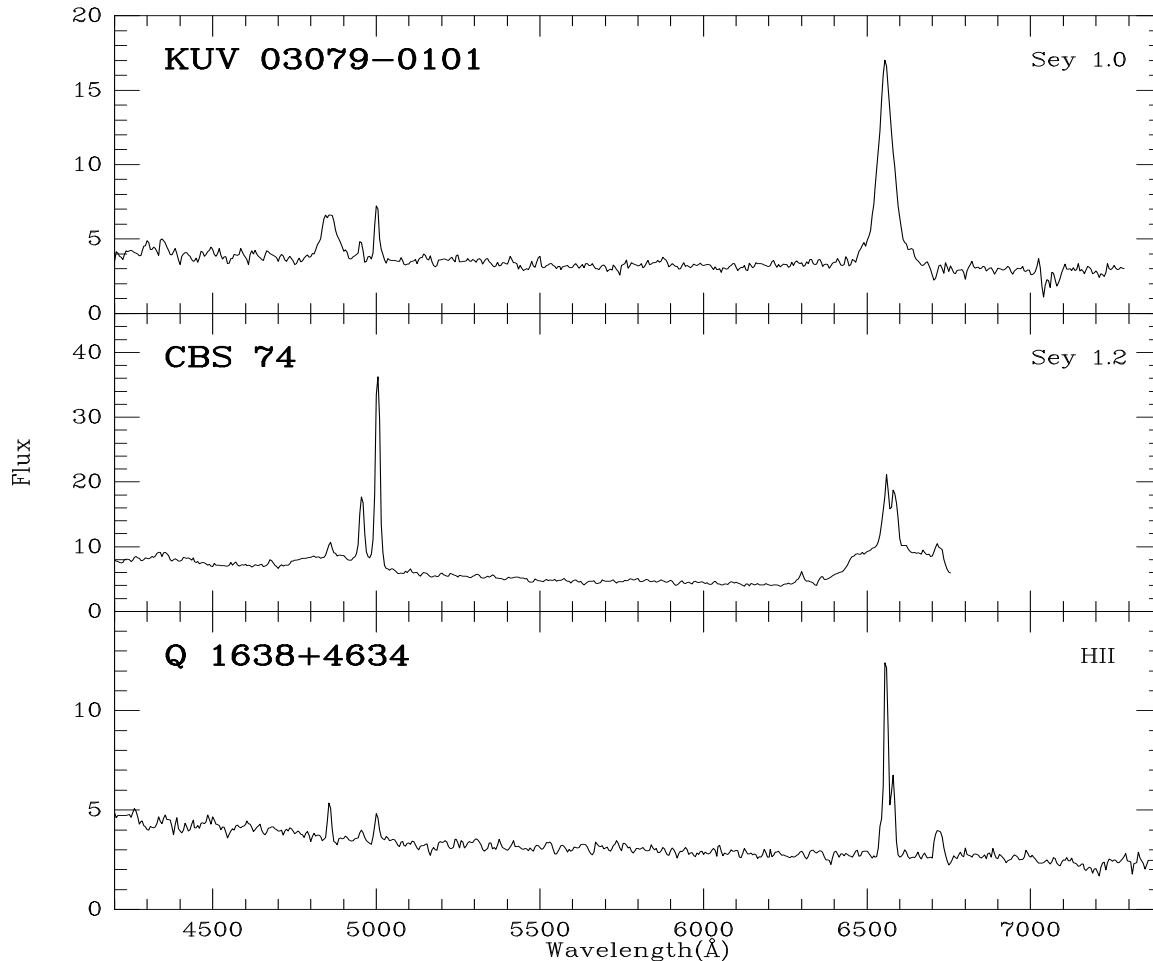


Fig. 3. Same as in Fig. 2 for three additional objects.

2.0) suggested that it is a HII region. This is confirmed by our spectrum (Fig. 8) which shows narrow emission lines (FWHM $< 225 \text{ km s}^{-1}$) with $\lambda 6584/\text{H}\alpha = 0.12$.

KUV 15519+2144 is a Seyfert 2 galaxy according to Wagner & Swanson (1990). Our spectrum (Fig. 8) shows it to be a HII region, with narrow (FWHM $< 185 \text{ km s}^{-1}$) emission lines and $\lambda 6584/\text{H}\alpha = 0.11$. A $\lambda 6300$ emission line is observed with $\lambda 6300/\text{H}\alpha = 0.02$

Q 1619+3752, an emission line galaxy according to Schneider et al. (1994), is classified as a HII region, as it shows narrow emission lines ($< 240 \text{ km s}^{-1}$ FWHM) and $\lambda 5007/\text{H}\beta = 2.56$ (Fig. 6).

EXO 1622.0+2611. An AGN for Giommi et al. (1991), this is a Seyfert 1 galaxy, as it presents a broad $\text{H}\alpha$ component (1770 km s^{-1} FWHM) (Fig. 8).

Q 1624+4628. An emission line galaxy according to Schneider et al. (1994), it is a HII region, with narrow ($< 195 \text{ km s}^{-1}$ FWHM) emission lines and $\lambda 6584/\text{H}\alpha = 0.40$ (Fig. 8).

Q 1638+4634. An emission line galaxy according to Schneider et al. (1994), it is a HII region, with $\lambda 5007/\text{H}\beta = 0.86$ and $\lambda 6584/\text{H}\alpha = 0.40$ (Fig. 3).

Kaz 110. The emission-line gas in this object was shown to be ionized by hot stars (Kazarian & Tamazian, 1993). Our spectra (Fig. 4) confirm this result, the measured line ratios being: $\lambda 5007/\text{H}\beta = 2.83$ and $\lambda 6584/\text{H}\alpha = 0.09$.

PKS 1903-80. This flat spectrum radio source (Quiniento & Cersosimo, 1993) was identified with a 19.0 mag QSO by Anguita et al. (1979). The identification was confirmed by an accurate radioposition mea-

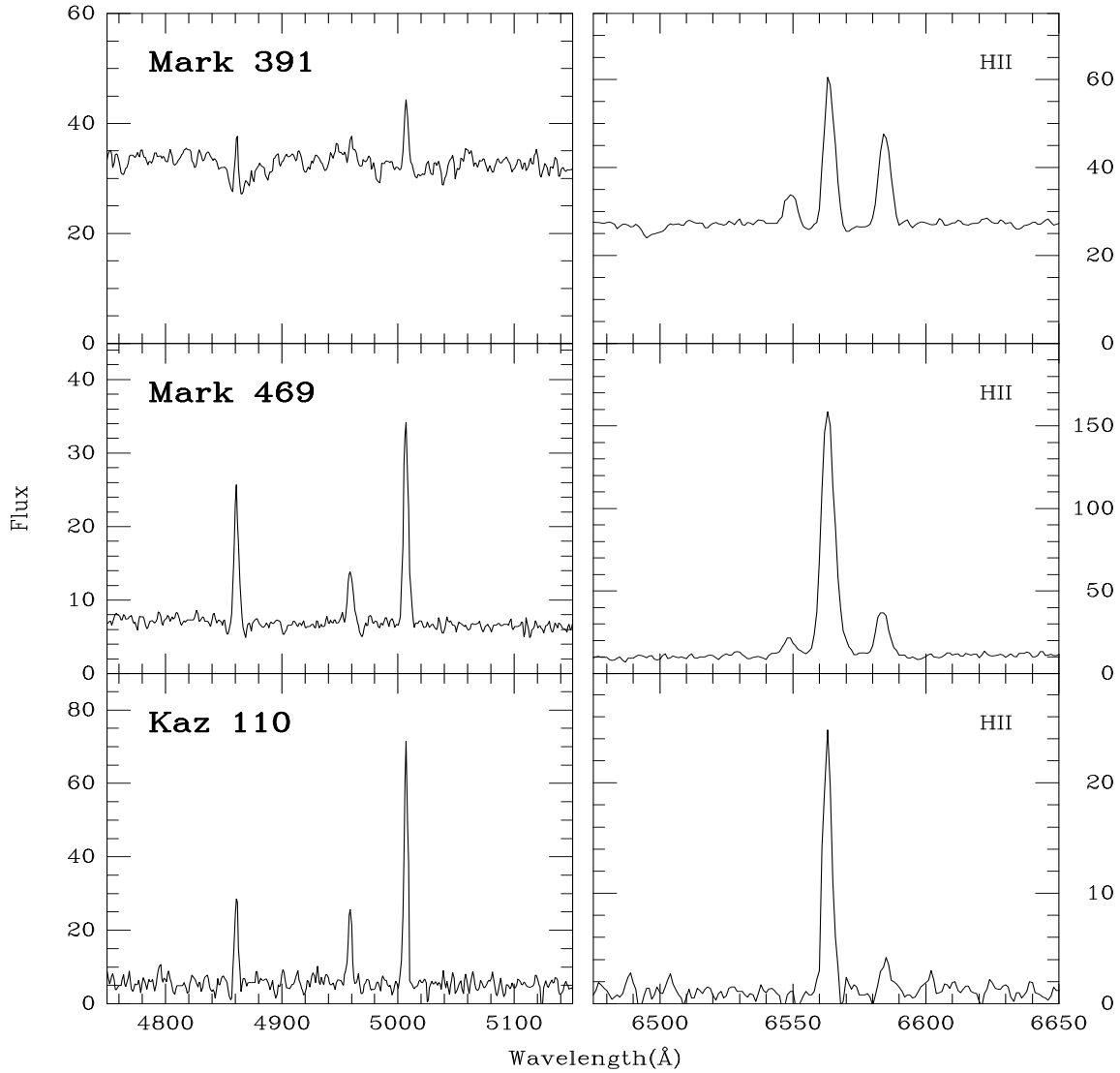


Fig. 4. Blue and red high dispersion spectra (resolution $\sim 3.4 \text{ \AA}$), in the rest frame, of three objects observed with the 1.93m OHP telescope. The fluxes are in units of $10^{-16} \text{ erg s}^{-1} \text{ cm}^{-2} \text{ \AA}^{-1}$.

surement (Russel et al., 1992). It is indeed a QSO at $z = 1.756$ (Fig. 1). The emission line fluxes are 57 and $25 \text{ } 10^{-16} \text{ erg s}^{-1} \text{ cm}^{-2}$ for $\text{CIV}\lambda 1550$ and $\text{CIII}\lambda 1909$ respectively.

RN 73 (Ryle & Neville, 1962) = 8C 2037+880 (Rees, 1990) was identified with a 17.5 mag emission line galaxy (Penston, 1971). Our spectra (Fig. 5) show a weak, broad ($\text{FWHM} \sim 1590 \text{ km s}^{-1}$) $\text{H}\alpha$ component, but no broad $\text{H}\beta$ component: this object is a Seyfert 1.9 galaxy. However, the ratio $\lambda 6584/\text{H}\alpha_{\text{narrow}} = 0.37$ is low for a Seyfert galaxy. Halliday (1977) published an accurate radiomap

for this source; its position, as measured on this map ($\alpha_{1950} = 20^{\text{h}}36^{\text{m}}44^{\text{s}}$, $\delta_{1950} = 88^{\circ}01'58''$), is about 20 arcsec away from the position of the galaxy, suggesting that the radiostructure and the galaxy are not to be related.

Q 2233+0123. An emission line galaxy according to Schneider et al. (1994), it is a Seyfert 1, having a strong and broad ($\text{FWHM} \sim 5500 \text{ km s}^{-1}$) $\text{H}\alpha$ component (Fig. 9). The profile of this line deviates significantly from a Gaussian, having a flat top.

Q 2257+0221 is an emission line galaxy according to Schneider et al. (1994). It is a Seyfert 2 having broad

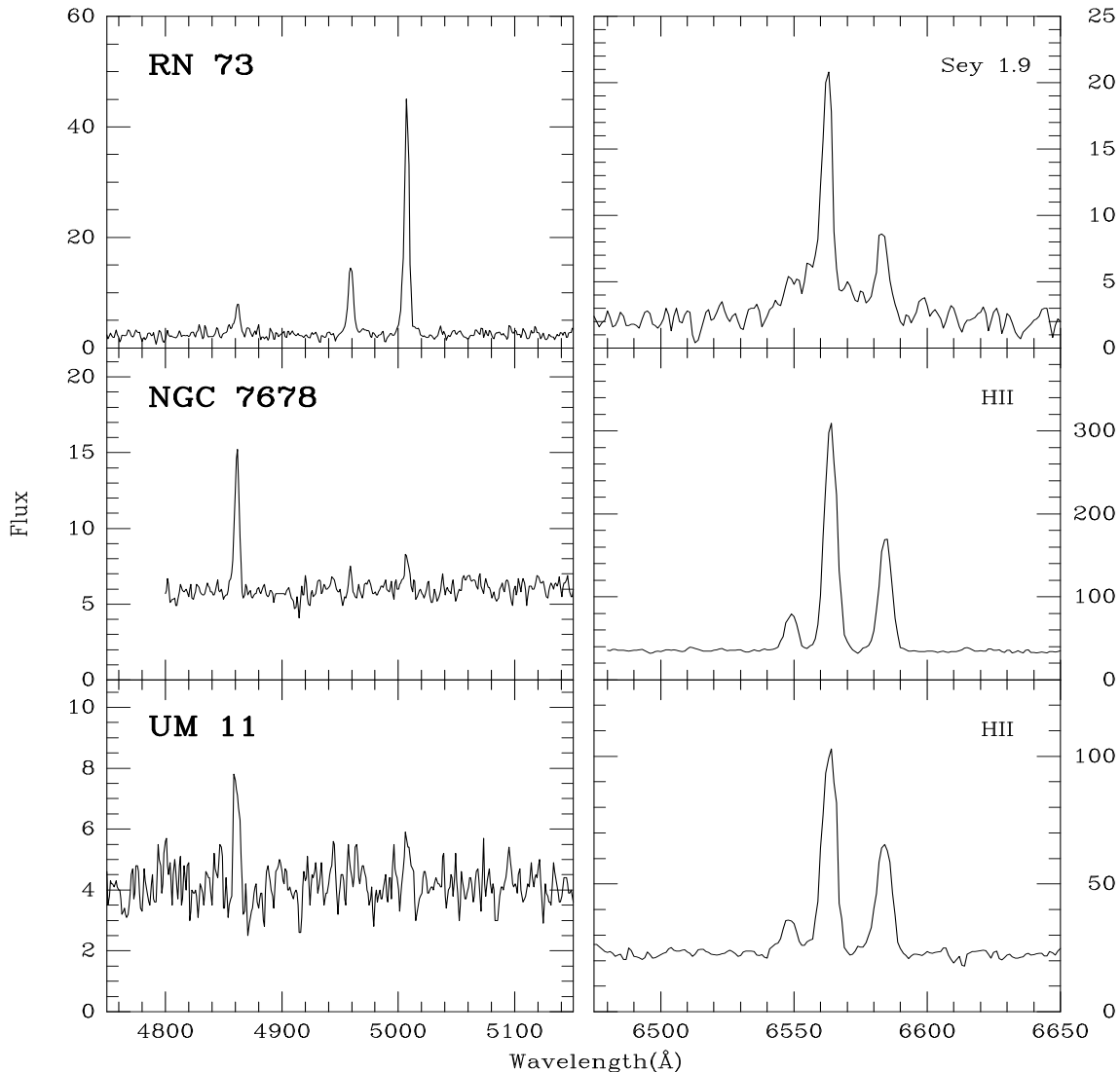


Fig. 5. Same as in Fig. 4 for three additional objects.

(FWHM $\sim 500 \text{ km s}^{-1}$), asymmetrical [OIII] lines, that are much stronger than $\text{H}\beta$ ($\lambda 5007/\text{H}\beta \sim 17$) (Fig. 6).

NGC 7678 = Kaz 336 (Kazarian & Kazarian, 1980). Although classified as a Seyfert 2 galaxy by Kazarian (1993), this is a HII region with $\lambda 6584/\text{H}\alpha = 0.52$, $\lambda 5007/\text{H}\beta = 0.25$ and linewidth $< 260 \text{ km s}^{-1}$ FWHM (Fig. 5).

E 2344+184 is a spiral galaxy (Hutchings & Neff, 1992). According to Margon et al. (1985), it is an emission line galaxy with a strong $\lambda 6584$ emission line. Our low signal-to-noise blue spectrum (Fig. 6) shows a strong

$\lambda 5007$ line ($\lambda 5007/\text{H}\beta > 6$), so it is most probably a Seyfert 2 galaxy.

UM 11. Terlevich et al. (1991) gave line ratios: $\lambda 6584/\text{H}\alpha = 1.23$ and $\lambda 5007/\text{H}\beta = 0.83$, suggesting that this object is a Liner; our spectra (Fig. 5) give $\lambda 6584/\text{H}\alpha = 0.56$ and $\lambda 5007/\text{H}\beta \sim 0.5$ (with linewidth $< 300 \text{ km s}^{-1}$ FWHM) showing that it is a HII region instead.

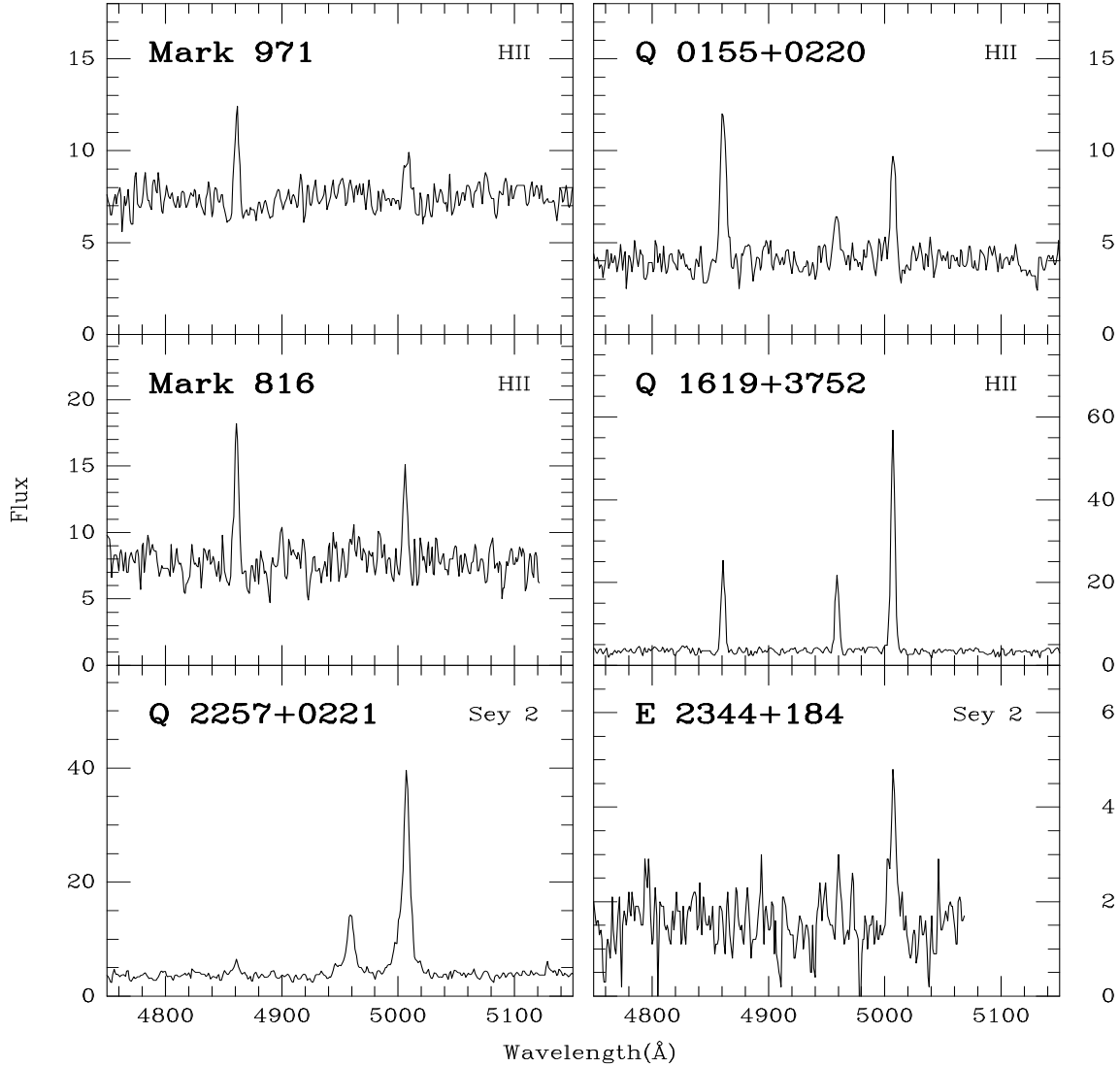


Fig. 6. Blue high dispersion spectra (resolution $\sim 3.4 \text{ \AA}$), in the rest frame, for six objects observed with the 1.93m telescope. The fluxes are in units of $10^{-16} \text{ erg s}^{-1} \text{ cm}^{-2} \text{ \AA}^{-1}$.

4. Conclusions

We have observed 37 AGN candidates and classified them on the basis of their spectroscopic properties; the line intensities and widths were obtained by fitting the spectra with Gaussian components. We concluded that three of the observed objects are confirmed QSOs, one is a BL Lac object, nine are Seyfert 1 galaxies, four are Seyfert 2s, while twenty are HII regions.

Acknowledgements. We are grateful to Dr. M. Viton for having allowed us to take the low dispersion spec-

trum of CBS 74 during his observing run. This research has made use of the NASA/IPAC extragalactic database (NED) which is operated by the Jet Propulsion Laboratory, Caltech, under contract with the National Aeronautics and Space Administration. A. C. Gonçalves acknowledges support from the JNICT during the course of this work, in the form of a PRAXIS XXI PhD. grant (PRAXIS XXI/BD/5117/95).

References

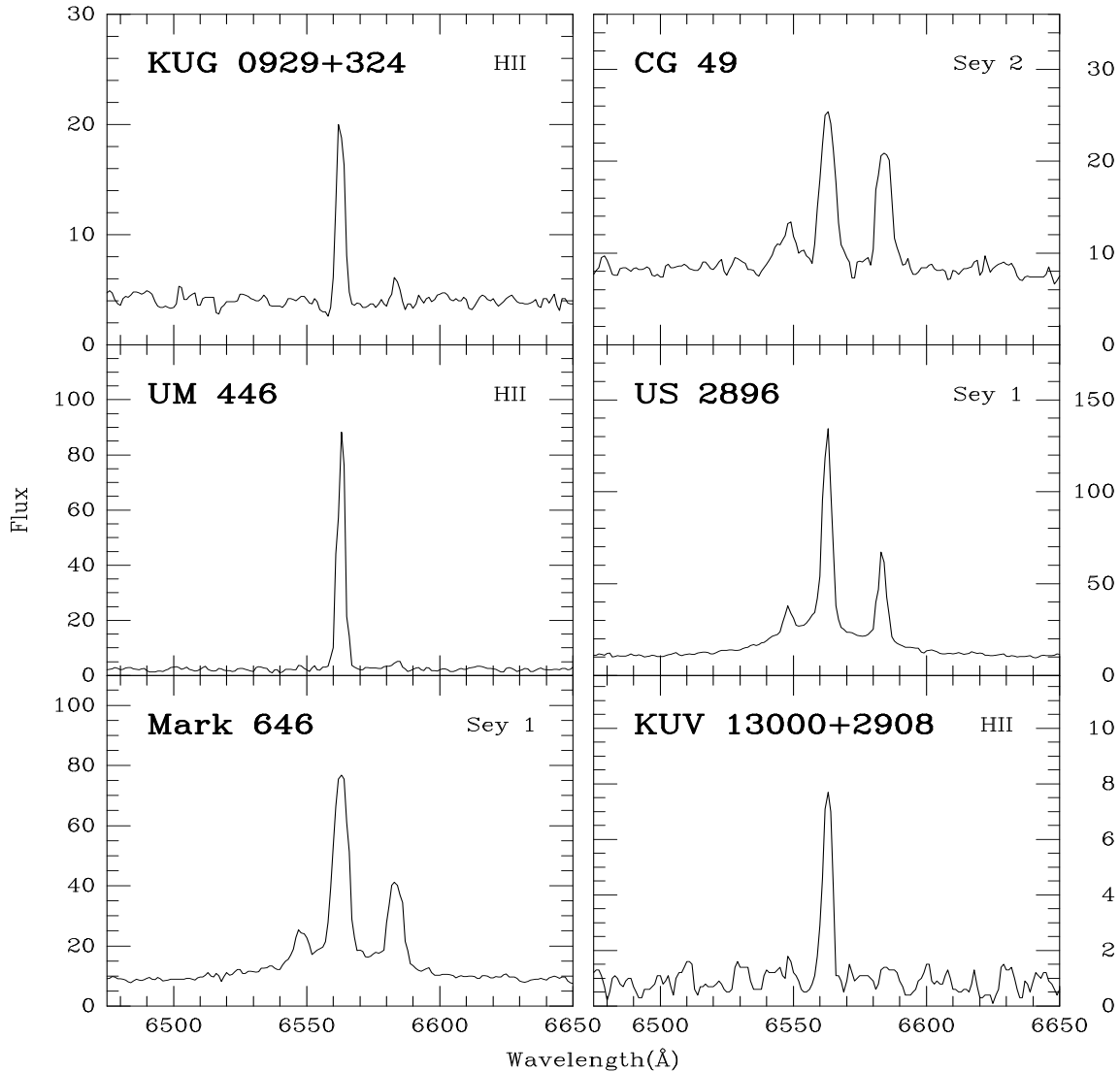


Fig. 7. Red high dispersion spectra (resolution $\sim 3.4 \text{ \AA}$), in the rest frame, for six objects observed with the 1.93m telescope. The fluxes are in units of $10^{-16} \text{ erg s}^{-1} \text{ cm}^{-2} \text{ \AA}^{-1}$.

- Afanasev V. L., Denisjuk E. K., Lipovetski V. A., 1979, *Soviet Astron. Letters* 5, 144
- Afanasev V. L., Lipovetski V. A., Markarian B. E., Stepanian D. A., 1980, *Astrophysics* 16, 119.
- Anguita C., Campusano L. E., Torres C., Pedreros M., 1979, *AJ* 84, 718
- Arakelian M. A., Dibai E. A., Esipov V. F., 1972, *Astrophysics* 8, 197
- Augarde R., Chalabaev A., Comte G., Kunth D., Machara H., 1994, *A&AS* 104, 259
- Bade N., Fink H. H., Engels D. et al., 1995, *A&AS* 110, 649
- Berger J., Cordoni J. P., Fringant A.-M. et al., 1991, *A&AS* 87, 389
- Bolton J. G., Ekers J., 1966, *Aust. J. Phys.* 19, 275
- Bothun F. D., Margon B., Balick B., 1984, *PASP* 96, 583
- Bowen D. V., Osmer S. J., Blades J. C. et al., 1994, *AJ* 107, 481
- Brotherton M. S., Wills B. J., Steidel C. C., Sargent W. L. W., 1994, *ApJ* 423, 131
- Chaffee F. H., Foltz C. B., Hewett P. C. et al., 1991, *AJ* 102, 461
- Chen K., Halpern J. P., 1989, *ApJ* 344, 115
- Condon J. J., Hicks P. D., Jauncey D. L., 1977, *AJ* 82, 692

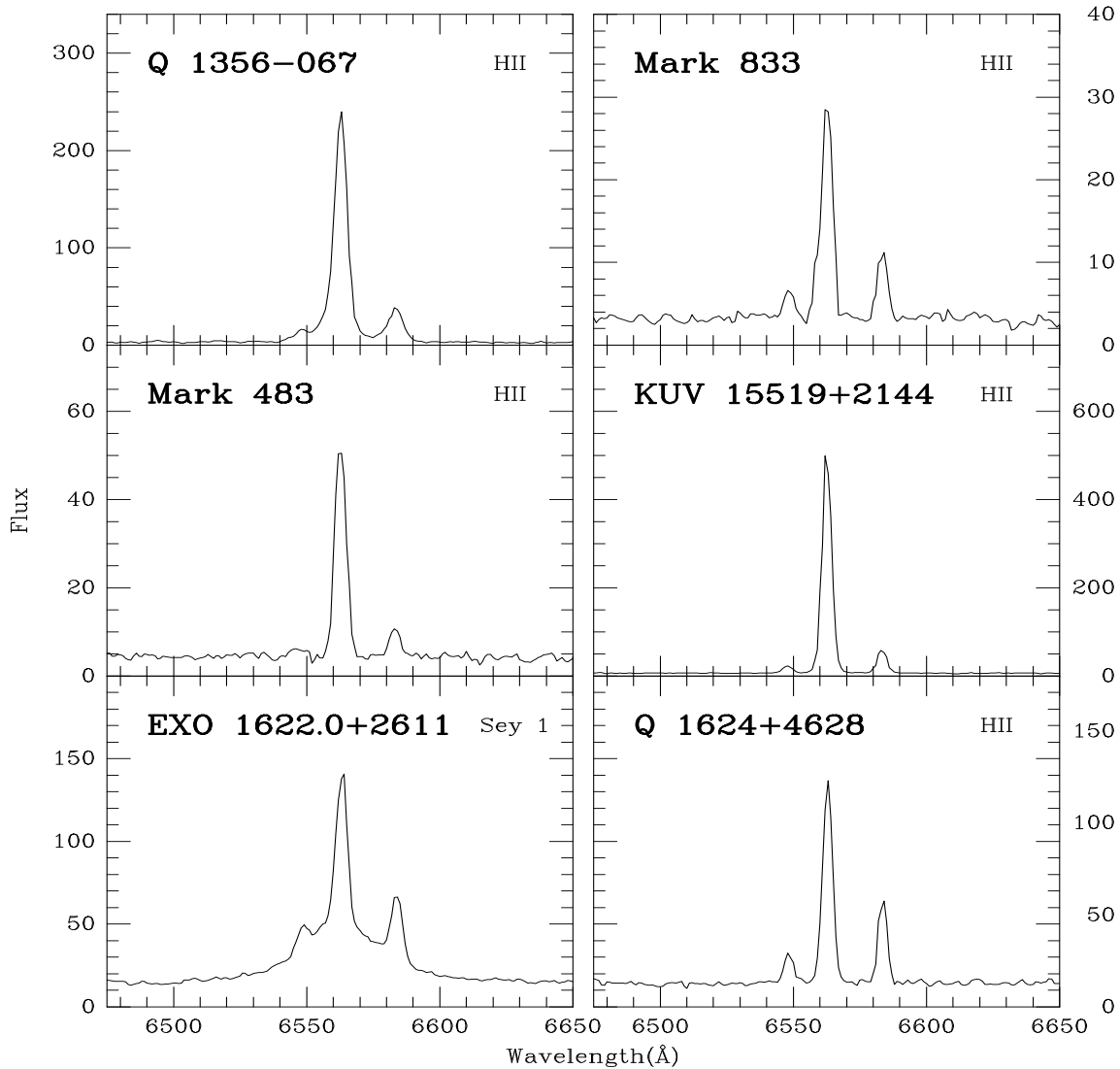


Fig. 8. Same as in Fig. 7 for six additional objects.

Dekker H., D'Odorico S., Arsenault R., 1988, *A&A* 189, 353
 Denisyuk E. K., Lipovetski V. A., 1984, *Astrophysics* 20, 290
 Eracleous M., Halpern J. P., 1994, *ApJS* 90, 1
 Everett M. E., Wagner R. M., 1995, *PASP* 107, 1059
 Giommi P., Tagliaferri G., Beuermann K. et al., 1991, *ApJ* 378, 77
 Goldschmidt P., Miller L., La Franca F., Cristiani S., 1992, *MNRAS* 256, 65P
 Gower J. F. R., Scott P. F., Wills D., 1967, *Mem. RAS* 71, 49
 Green R. F., Schmidt M., Liebert J., 1986, *ApJS* 61, 305
 Gregory P. C., Condon J. J., 1991, *ApJS* 75, 1011
 Halliday J., 1977, *MNRAS* 179, 111
 Huang K. L., Usher P. D., 1984, *ApJS* 56, 393

Huchra J. P., 1977, *ApJS* 35, 171
 Hunstead R. W., 1971, *MNRAS* 152, 277
 Hunstead R. W., 1972, *MNRAS* 157, 367
 Hutchings J. B., Neff S. G., 1992, *AJ* 104, 1
 Izotov Y. I., Lipovetski V. A., Guseva N. G. et al., 1993, *A&A* Trans. 3, 197
 Jauncey D. L., Wright A. E., Peterson B. A., Condon J. J., 1978, *ApJ* 219, L1
 Kazarian M. A., 1979, *Astrophysics* 15, 1
 Kazarian M. A., 1993, *Astrophysics* 36, 217
 Kazarian M. A., Kazarian E. S., 1980, *Astrophysics* 16, 7
 Kazarian M. A., Tamazian V. S., 1993, *Astrophysics* 36, 222

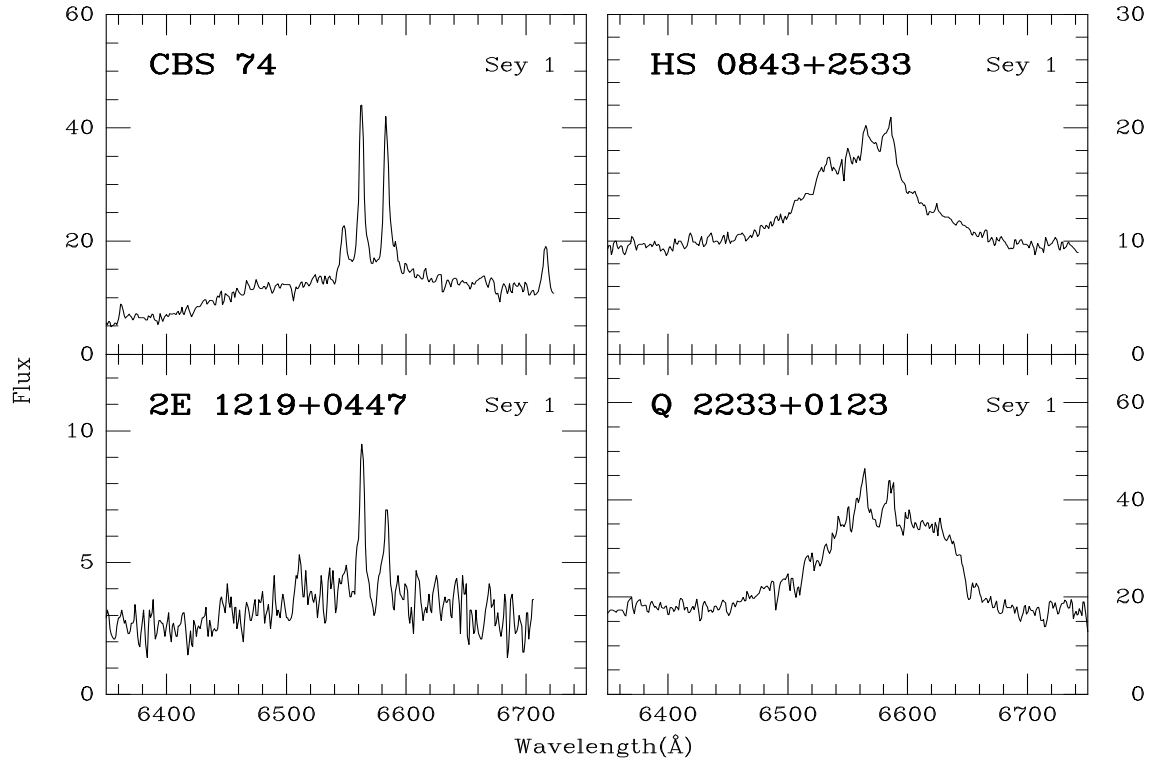


Fig. 9. Same as in fig. 7 for four additional objects.

- Kondo M., Noguchi T., Machara H., 1984, *Ann. Tokyo Astron. Obs.* 20, 130
- Lemaître G., Kohler D., Lacroix D., Meunier J.-P., Vin A., 1989, *A&A* 228, 546
- Lipovetski V. A., Shapovalova A. I., Stepanian D. A., Erastova L. K., 1989, *Astrophysics* 31, 665
- MacAlpine G. M., Williams G. A., 1981, *ApJS* 45, 113
- MacAlpine G. M., Smith S. B., Lewis D. W., 1977, *ApJS* 34, 95
- Margon B., Downes R. A., Chanan G. A., 1985, *ApJS* 59, 23
- Markarian B. E., Lipovetski V. A., 1971, *Astrophysics* 7, 299
- Markarian B. E., Lipovetski V. A., 1972, *Astrophysics* 8, 89
- Markarian B. E., Lipovetski V. A., 1973, *Astrophysics* 9, 283
- Markarian B. E., Lipovetski V. A., 1974, *Astrophysics* 10, 185
- Markarian B. E., Lipovetski V. A., 1976, *Astrophysics* 12, 429
- Markarian B. E., Lipovetski V. A., Stepanian D. A., 1977a, *Astrophysics* 13, 116
- Markarian B. E., Lipovetski V. A., Stepanian D. A., 1977b, *Astrophysics* 13, 215
- Markarian B. E., Lipovetski V. A., Stepanian D. A., 1979, *Astrophysics* 15, 130
- Markarian B. E., Lipovetski V. A., Stepanian D. A., 1980, *Astrophysics* 16, 1
- Markarian B. E., Lipovetski V. A., Stepanian D. A., 1984, *Astrophysics* 20, 581
- Markarian B. E., Erastova L. K., Lipovetski V. A., Stepanian D. A., Shapovalova A. I., 1985, *Astrophysics* 22, 127
- Markarian B. E., Erastova L. K., Lipovetski V. A., Stepanian D. A., Shapovalova A. I., 1988, *Astrophysics* 28, 14
- Massey P., Strobel K., Barnes J. V., Anderson E., 1988, *ApJ* 328, 315
- Miley G. K., Miller J. S., 1979, *ApJ* 228, L55
- Mitchell K. J., Warnock A., Usher P. D., 1984, *ApJ* 287, L3
- Noguchi T., Machara H., Kondo M., 1980, *Ann. Tokyo Astron. Obs.* 18, 55
- Oke J. B., 1974, *ApJS* 27, 21
- Oke J. B., Gunn J. E., 1983, *ApJ* 266, 713
- Penston M. V., 1971, *ApJ* 170, 395
- Pesch P., Sanduleak N., 1983, *ApJS* 51, 171
- Pesch P., Sanduleak N., 1986, *ApJS* 60, 543
- Pesch P., Sanduleak N., 1988, *ApJS* 66, 297
- Pesch P., Sanduleak N., 1989, *ApJS* 70, 163
- Peterson B. M., Fricke K., Biermann P., 1981, *PASP* 93, 281
- Quintero Z. M., Cersosimo J. C., 1993, *A&AS* 97, 435
- Rees N., 1990, *MNRAS* 244, 233
- Russel J. L., Jauncey D. L., Harvey B. R. et al., 1992, *AJ* 103, 2090
- Ryle M., Neville A. C., 1962, *MNRAS* 125, 39
- Salzer J. J., MacAlpine G. M., Boroson T. A., 1989, *ApJS* 70, 447

- Salzer J. J., Moody J. W., Rosenberg J. L., Gregory S. A.,
Newberry M. V., 1995, *AJ* 109, 2376
- Sanduleak N., Pesch P., 1984, *ApJS* 55, 517
- Sanduleak N., Pesch P., 1987, *ApJS* 63, 809
- Sanduleak N., Pesch P., 1990, *ApJS* 72, 291
- Schneider D. P., Schmidt M. S., Gunn J. E., 1994, *AJ* 107,
1245
- Shimmins A. J., Bolton J. G., Wall J. V., 1975, *Aust. J. Phys.*
Astrophys. Suppl. 34, 63
- Shuder J. M., Osterbrock D. E., 1981, *ApJ* 250, 55
- Steiner J. E., 1981, *ApJ* 250, 469
- Stone R. P. S., 1977, *ApJ* 218, 767
- Takase B., Miyauchi-Isobe N., 1984, *Ann. Tokyo Astron. Obs.*
19, 595
- Takase B., Miyauchi-Isobe N., 1985, *Ann. Tokyo Astron. Obs.*
21, 127
- Takase B., Miyauchi-Isobe N., 1991a, *Pub. Nat. Obs. Japan* 2,
37
- Takase B., Miyauchi-Isobe N., 1991b, *Pub. Nat. Obs. Japan* 2,
239
- Terlevich R., Melnick J., Masegosa J., Moles M., Copetti M.
V. F., 1991, *A&AS* 91, 285
- Veilleux S., Osterbrock D. E., 1987, *ApJS* 63, 295
- Véron-Cetty M.-P., Véron P., 1985, *ESO Scientific Report No*
4
- Véron-Cetty M.-P., Véron P., 1986, *A&AS* 65, 241
- Véron-Cetty M.-P., Véron P., 1996, *A&AS* 115, 97
- Véron P., Gonçalves A. C., Véron-Cetty M.-P., 1997, *A&A* 319,
52
- Wagner R. M., Swanson S. R., 1990, *AJ* 99, 330
- Wagner R. M., Sion E. M., Liebert J., Stanfield S. G., 1988,
ApJ 328, 213
- Wegner G., McMahan R. K., 1988, *AJ* 96, 1933
- Wills B. J., Browne I. W. A., 1986, *ApJ* 302, 56
- Wills D., Wills B. J., 1976, *ApJS* 31, 143
- Winkler H., 1992, *MNRAS* 257, 677

| Name | α | δ | z | mag | old class. | our class. | Ref. |
|-------------------|-------------|--------------|-------|------|------------|------------|------|
| 4C 12.05 | 00 35 41.98 | 12 11 03.6 | – | 17.5 | ? | Q | (25) |
| Mark 1147 | 00 45 57.94 | 10 03 56.9 | 0.036 | 15.7 | S1 | HII | (18) |
| Mark 971 | 01 01 32.79 | 35 18 07.8 | 0.085 | 16.5 | S? | HII | (16) |
| Mark 998 | 01 30 02.04 | – 02 20 11.9 | 0.078 | 16.0 | S? | HII | (17) |
| Q 0155 + 0220 | 01 55 47.90 | 02 20 26.3 | 0.066 | 16.7 | ? | HII | (23) |
| Mark 596 | 02 40 12.67 | 07 23 09.5* | 0.038 | 14.8 | S? | S2 | (13) |
| KUV 03079 – 0101 | 03 07 54.83 | – 01 01 10.3 | 0.080 | 16.3 | ? | S1.0 | (7) |
| CBS 74 | 08 29 11.46 | 37 17 49.1 | 0.091 | 17. | S | S1.2 | (21) |
| HS 0843 + 2533 | 08 43 56.47 | 25 33 14.7 | 0.050 | 16.8 | S1 | S1 | – |
| Mark 391 | 08 51 32.38 | 39 43 45.5 | 0.013 | 14.1 | S? | HII | (11) |
| KUG 0929 + 324 | 09 29 01.90 | 32 26 59.9* | 0.005 | 17.5 | ? | HII | (24) |
| CG 49 | 09 58 07.76 | 31 26 44.7 | 0.042 | 16.4 | S2 | S2 | (20) |
| UM 446 | 11 39 12.06 | – 01 37 27.1 | 0.005 | 17.3 | ? | HII | (8) |
| US 2896 | 11 42 33.73 | 31 03 56.5 | 0.060 | 16.0 | S1.5 | S1 | (22) |
| Mark 646 | 12 03 17.01 | 35 27 27.5 | 0.054 | 15.3 | S | S1 | (14) |
| 2E 1219 + 0447 | 12 19 04.62 | 04 47 04.3 | 0.094 | 16.8 | ? | S1 | (3) |
| KUV 13000 + 2908 | 13 00 01.52 | 29 07 37.0 | 0.023 | 16.1 | S2 | HII | (7) |
| Q 1356 – 067 | 13 56 44.90 | – 06 07 43.8 | 0.072 | 16.2 | S? | HII | – |
| Mark 469 | 14 16 12.98 | 34 35 46.0 | 0.069 | 16.0 | ? | HII | (12) |
| PKS 1420 – 27 | 14 19 55.50 | – 27 14 20.8 | – | 18. | Q? | Q | (2) |
| Mark 816 | 14 31 40.78 | 52 59 26.8 | 0.089 | 16.5 | S? | HII | (15) |
| PKS 1437 – 153 | 14 37 11.31 | – 15 18 58.9 | – | 19. | Q? | BL | (4) |
| Mark 833 | 14 55 59.69 | 35 24 05.4 | 0.040 | 16.0 | S? | HII | (15) |
| Mark 483 | 15 28 41.48 | 34 05 53.3 | 0.048 | 16.4 | HII | HII | (12) |
| KUV 15519 + 2144 | 15 51 53.33 | 21 43 42.9 | 0.040 | 15.8 | S2 | HII | (7) |
| Q 1619 + 3752 | 16 19 55.81 | 37 52 36.3 | 0.034 | 17.3 | ? | HII | (23) |
| EXO 1622.0 + 2611 | 16 22 05.33 | 26 11 23.9 | – | 16.1 | S? | S1 | – |
| Q 1624 + 4628 | 16 24 34.76 | 46 28 48.2 | 0.030 | 16.1 | ? | HII | (23) |
| Q 1638 + 4634 | 16 38 50.52 | 46 34 38.8 | 0.059 | 16.4 | ? | HII | (23) |
| Kaz 110 | 16 57 16.83 | 69 09 08.0 | 0.053 | 17.2 | HII | HII | (5) |
| PKS 1903 – 80 | 19 03 56.16 | – 80 14 59.8 | – | 19.0 | Q? | Q | (1) |
| RN 73 | 20 36 08.47 | 88 02 05.4 | 0.047 | 17.5 | ? | S1.9 | (19) |
| Q 2233 + 0123 | 22 33 08.78 | 01 24 00.2 | 0.058 | 16.6 | ? | S1 | (23) |
| Q 2257 + 0221 | 22 57 00.37 | 02 21 29.8 | 0.048 | 16.7 | ? | S2 | (23) |
| NGC 7678 | 23 25 57.91 | 22 08 44.7 | 0.012 | 15.3 | S2 | HII | (6) |
| E 2344 + 184 | 23 44 53.30 | 18 28 10.8 | 0.138 | 15.9 | ? | S2 | (10) |
| UM 11 | 23 50 45.22 | 03 26 22.3* | 0.038 | 16.0 | S | HII | (9) |

Table 3. This table gives for each of the observed objects: the name (col. 1), the B1950 optical position measured on the Digitized Sky Survey (col. 2 and 3), where the the r.m.s. error is 0.6 arcsec in each coordinate; “*” indicates objects with larger errors because of their location near one edge of the Schmidt plate (Véron-Cetty & Véron, 1996), the published redshift (col. 4), the magnitude (col. 5), the old spectral classification: S2: Seyfert 2, S1: Seyfert 1, HII: HII region, Q: Quasar, ?: unknown (col. 6), and our classification (col. 7). References for the finding charts (col. 8): (1) Anguita et al. (1979), (2) Bolton & Ekers (1966), (3) Bowen et al. (1994), (4) Condon et al. (1977), (5) Kazarian (1979), (6) Kazarian & Kazarian (1980), (7) Kondo et al. (1984), (8) MacAlpine & Williams (1981), (9) MacAlpine et al. (1977), (10) Margon et al. (1985), (11) Markarian & Lipovetski (1971), (12) Markarian & Lipovetski (1972), (13) Markarian & Lipovetski (1973), (14) Markarian & Lipovetski (1974), (15) Markarian & Lipovetski (1976), (16) Markarian et al. (1977a), (17) Markarian et al. (1977b), (18) Markarian et al. (1979), (19) Penston (1971), (20) Pesch & Sanduleak (1983), (21) Pesch & Sanduleak (1986), (22) Sanduleak & Pesch (1984), (23) Schneider et al. (1994), (24) Takase & Miyauchi-Isobe (1985), (25) Wills & Wills (1976).

| Name | z | V (kms ⁻¹) | FWHM (kms ⁻¹) | $\lambda 5007$ H β | H β | V (kms ⁻¹) | FWHM (kms ⁻¹) | $\lambda 6584$ H α | H α | Spectral type |
|-----------------|--------|---------------------------|------------------------------|-----------------------------|-----------|---------------------------|------------------------------|------------------------------|------------|------------------|
| Mark 1147 | 0.0364 | 14 | (780) | 2.18 | 2.3 | 11 | (635) | 0.24 | 11.4 | HII |
| Mark 971 | 0.0823 | 15 | 280 | 0.41 | 5.6 | – | – | – | – | HII |
| Mark 998 | 0.0761 | – | – | – | – | 22 | (580) | 0.23 | 10.3 | HII |
| Q 0155 + 0220 | 0.0651 | -1 | 325 | 0.71 | 8.4 | – | – | – | – | HII |
| Mark 596 | 0.0388 | -16 | (960) | > 5.0 | < 0.6 | 45 | (720) | 1.14 | 2.2 | S2 |
| KUV 03079–0101 | 0.0807 | -15 | (860) | > 10.0 | < 0.4 | – | – | – | – | S1.0 |
| | | -29 | 3360 | – | 3.1 | -28 | 2570 | – | 12.2 | |
| CBS 74 | 0.0920 | 143 | (945) | 15.6 | 1.9 | -10 | 260 | 0.89 | 27.8 | S1.2 |
| | | 1485 | 14500 | – | 2.3 | 1092 | 12200 | – | 10.4 | |
| HS 0843+2533 | 0.0507 | – | – | – | – | 90 | 475 | 1.6 | 2.5 | S1 |
| | | – | – | – | – | -70 | 4850 | – | 7.3 | |
| Mark 391 | 0.0133 | 9 | 210 | 1.21 | 9.9 | 45 | 225 | 0.55 | 36.7 | HII |
| KUG 0929+324 | 0.0158 | – | – | – | – | -6 | 150 | 0.10 | 17.6 | HII |
| CG 49 | 0.0438 | – | – | – | – | 15 | 300 | 0.79 | 17.4 | S2 |
| UM 446 | 0.0061 | – | – | – | – | 9 | 160 | 0.04 | 79.8 | HII |
| US 2896 | 0.0594 | – | – | – | – | -3 | 185 | 0.43 | 103 | S1 |
| | | – | – | – | – | -120 | 2100 | – | 12.3 | |
| Mark 646 | 0.0536 | – | – | – | – | 0 | 280 | 0.46 | 62.8 | S1 |
| | | – | – | – | – | -16 | 2350 | – | 8.0 | |
| 2E 1219+0447 | 0.0947 | – | – | – | – | 3 | 225 | 0.54 | 5.5 | S1 |
| | | – | – | – | – | 222 | 8440 | – | 1.6 | |
| KUV 13000+2908 | 0.0223 | – | – | – | – | 3 | 185 | < 0.1 | 7.0 | HII |
| Q 1356-067 | 0.0746 | – | – | – | – | 6 | 280 | 0.16 | 226 | HII |
| Mark 469 | 0.0689 | -9 | 295 | 1.38 | 19.4 | 18 | 260 | 0.18 | 147 | HII |
| Mark 816 | 0.0887 | -19 | 240 | 0.63 | 10.5 | – | – | – | – | HII |
| Mark 833 | 0.0395 | – | – | – | – | -8 | 225 | 0.30 | 25.7 | HII |
| Mark 483 | 0.0481 | – | – | – | – | -5 | 225 | 0.12 | 48.3 | HII |
| KUV 15519+2144 | 0.0392 | – | – | – | – | -9 | 185 | 0.11 | 483 | HII |
| Q 1619+3752 | 0.0331 | -3 | 240 | 2.56 | 20.4 | – | – | – | – | HII |
| EXO 1622.0+2611 | 0.0394 | – | – | – | – | 15 | 225 | 0.40 | 93.0 | S1 |
| | | – | – | – | – | 12 | 1770 | – | 33.0 | |
| Q 1624+4628 | 0.0301 | – | – | – | – | 6 | 195 | 0.40 | 124 | HII |
| Q 1638+4634 | 0.0581 | 10 | (720) | 0.86 | 1.8 | 36 | (625) | 0.40 | 10.3 | HII |
| Kaz 110 | 0.0527 | -5 | 225 | 2.83 | 22.9 | 9 | 170 | 0.09 | 23.1 | HII |
| RN 73 | 0.0491 | 18 | 310 | 7.4 | 5.4 | -16 | 185 | 0.37 | 16.3 | S1.9 |
| | | – | – | – | – | -34 | 1590 | – | 3.1 | |
| Q 2233+0123 | 0.0566 | – | – | – | – | 15 | 290 | 0.60 | 8.5 | S1 |
| | | – | – | – | – | 1080 | 5500 | – | 21.3 | |
| Q 2257+0221 | 0.0466 | 3 | 495 | 16.7 | 1.9 | – | – | – | – | S2 |
| NGC 7678 | 0.0116 | 12 | 270 | 0.25 | 9.5 | 45 | 250 | 0.52 | 272 | HII |
| E 2344+184 | 0.1365 | 24 | 425 | > 6.0 | < 0.5 | – | – | – | – | S2 |
| UM 11 | 0.0390 | -8 | 310 | 0.46 | 3.8 | 21 | 290 | 0.56 | 80.2 | HII |

Table 4. Fitting profile analysis results (see text). Col. 2 gives the redshift used to deredshift the spectra, while col. 3 and 7 give the velocity of the lines as measured on the deredshifted spectra. Col. 6 and 10 give the peak intensity of the H β and H α lines respectively (in units of 10^{-16} erg s⁻¹ cm⁻² Å⁻¹). The FWHM are observed values, not corrected for the instrumental profile; values in parenthesis are from low dispersion spectra and are unresolved.